Visual Abstract

Microstructure characterization of sustainable light weight concrete using trapped air additions

A. A. Maaty
Structural Engineering Dept,Faculty of Engineering, Tanta University, Egypt
saidmaaty@yahoo.com, http://orcid.org/0000-0002-3166-6556

Fryal M. Kamel, A.A. ELShami
Misr Higher Institute of Eng.&Tech, Elmansura, Egypt
engfryalkamel@yahoo.com, https://orcid.org/0000-0003-2302-3355
materialhnbrc@yahoo.com, http://orcid.org/0000-0002-9075-7669

ABSTRACT. Light-weight aggregate and trapped air additions (TAD) affect concrete performance and lead to the production of light-weight concrete (LWC). In this research, fourteen mixes were designed to study the effects of TAD type and content and pozzolanic material (PZ) type on the microstructure characterization of concrete. Aluminum powder (AP) and lightcrete (LC) were used as TAD with content equal to (0%, 0.25%, 0.50%, 0.57%). The PZ included silica fume (SF) and fly ash (FA) with content equal to 10% of the weight of cement. Tests were performed for compressive strength, density, SEM, EDS, XRD, and TGA/DTG. The results show that the compressive strength and density are reduced as TAD ratios are increased. On the other hand, the results of SEM and EDS showed that the production of calcium silicate hydrate (CSH) was reduced, but the pores and air voids were increased. However, the tests TGA/DTG performed showed that the hydration degree of the mix without TAD cement paste grew faster than the other mixes.

KEYWORDS. Light-weight concrete (LWC); Trapped air additions (TAD); Pozzolanic materials (PZ); Compressive strength; Density; Microstructure.

OPEN ACCESS

Citation: Maaty, A. A., Kamel, F. M., ELShami, A. A., Microstructure characterization of sustainable light weight concrete using trapped air additions, Frattura ed Integrità Strutturale, 62 (2022) 194-211.

Received: 10.06.2022
Accepted: 24.08.2022
Online first: 26.08.2022
Published: 01.10.2022

INTRODUCTION

Sustainable building methods and materials are required to ensure the construction industry's safe and clean future since they presently account for more than 7% of global carbon dioxide emissions. Construction experts and scholars have taken various approaches to solve the building industry's environmental challenges over the last few decades. The primary components of concrete (cement, fine aggregate, and coarse aggregate) were used to replace them with eco-friendly alternatives without compromising concrete's main mechanical and durability properties [1-3].

Light-weight concrete (LWC) is made by substituting natural aggregates for light-weight materials. Reducing weight is an essential aim in building and construction because it acts as a good thermal insulator and lowers construction costs and time [4, 5]. Researchers have focused on light-weight porous materials derived from industrial waste [6-8].
In general, the density of LWC is lower than 2000 kg/m^3 [9-12]. The LWC's air bubbles provide dense, lower-density concrete. For example, Alla Sai Krishna et al. in their research, mixed foam agents with different ratios (25%, 50%, and 75%) of fly ash by weight of cement achieved varying densities ranging from 800 kg/m^3 to 1600 kg/m^3 [11]. Manan Hashim et al. in their study focused on increasing the amount of two types of foaming agents (protein and synthetic-based) in the mixes from 30 to 112 kg/m^3, the concrete densities ranging from 600 kg/m^3 to 1200 kg/m^3 [13]. Marcin Kozlowski et al. used portland cement, W/C = 0.44, five mixes with fly ash and five mixes without, and foam agents in various percentages (0.5%, 1%, 1.5%, 2%, and 2.5%). As a result, the density changed from 400 to 1400 kg/m^3 [14].
The air-entraining agent can affect the workability of concrete, but this effect depends on the different environmental conditions and the type of use. Also, the fresh and hardened concrete have different air content and air void distribution according to the structure's evolution [15, 16].
Hussein Al-Kroom et al. [17] used crushed clay brick (CB) as coarse, fine, and powder aggregates. Ordinary Portland cement, SF, and SP were employed. In filler materials, CBP was used in different weight ratios (0 wt. %, 10 wt. %, 20 wt. %, and 30 wt. %) and air-entraining agent (AEA) was utilized in various weight ratios (0.25 wt. %, 0.5 wt. %, 0.75 wt. %, and 1 wt. %). As a result, the use of AEA in concrete reduced the density from 1870 kg/m^3 to 1746 kg/m^3, the compressive strength from 41 MPa to 34 MPa, and microstructural tests (SEM, XRD, TGA, and MIP) revealed that adding an AEA to concrete reduces the formation of CSH while increasing pores and air voids.
Muhammad Riaz et al. [18] used Portland cement, SF, SP, fine sand, expanded clay aggregate (ECA), foaming agent (FA), and water. Mixes (without SF) containing (0%, 10%, 15%, and 20%) FA. The compressive strength was 24.75, 21.10, 15.95, and 12.05 MPa; the dry density was reduced from (1525.8, 1362.5, 1253.5, and 1225.2 kg/m^3); and the total volume of pores was 25.68, 30.58, 36.90, and 39.74 %, respectively. However, the addition of SF improved the mechanical characteristics of the mixes. The maximum compressive strength was 28.2 MPa, the densities were (1577.7, 1403.5, 1291.9, and 1232.9 kg/m^3), and the total pore volume was respectively 22.18, 27.28, 32.67, and 35.13% [18]. H.K. Kim et al. Portland cement, the water-cement ratio (w/c) was at 0.47, and the sand–aggregate ratio (S/a) of normal and lightweight aggregate concrete was 0.48 and 0.32, respectively. For normal concrete, 100% river sand and crushed gravel were used. For lightweight aggregate concrete, 100% fine bottom ash and coarse expanded shale were used. The air entraining agent was used for lightweight aggregate concrete with four different weight percentages (0%, 0.5%, 1.0%, and 1.5%) of cement. As a result of this, The density of normal concrete was 2355 kg/m^3 in a (surface saturated dry) S.S.D. condition, but the density of lightweight concrete was 1800 kg/m^3. When a 1.0 % AE agent was employed, the density was 1553 kg/m^3, but when a 1.5 % AE agent was used, the density increased to 1659 kg/m^3. Meanwhile, under the O.D. condition, the density of lightweight concrete was 1213 kg/m^3 with a 1.0 % AE agent addition but increased to 1331 kg/m^3 with a 1.5 % AE agent addition. Normal concrete had a compressive strength of 40 MPa, which was reduced to 22 MPa with the addition of lightweight particles. The compressive strength of lightweight concrete was reduced to 8 MPa when the addition of AE agent was increased to 1.0% and increased to 11 MPa with 1.5% of added AE agent [19].
The advantages of LWC include fire resistance, acoustic insulation, and assistance to the green environment. Additionally, the higher-performing high-strength (LWC) aids in the creation of bridge girders with a large span [20, 21].
For architectural and practical design, LWC is better than ordinary concrete. LWC can be used in place of ordinary concrete in various applications, including high-rise building floors, columns, and walls; curtain walls; shell roofs; folded panels; bridge decks; and girders [22-24].
One of the deficiencies of LWC is that it contains more light-weight aggregate in the pressure region than natural concrete, and the light-weight porous aggregate can affect concrete strength and durability substantially [25, 26]. Although good LWC compaction is required, excessive vibration can easily cause segregation [27].
In this study, LWC was obtained using light-weight aggregates such as pumice and Addipore55 and ventilation with concrete air bubbles. This investigation also examined the effects of TAD type, content, and (PZ) type on the properties of LWC and how the voids produced by TAD affect the pressure strength and the density of LWC.

EXPERIMENTAL PROGRAM

Materials

Ordinary Portland Cement (OPC) grade 42.5 N is verified by Egyptian Standard Specifications (4756-1/2007). Laboratory testing confirmed the chemical composition and physical characteristics of the cement used (according to E.S.S. No. 2421/2005) [28], indicating effective concrete work. The specifications of the cement used in this investigation are shown in Tabs. 1 and 2. The cement content per cubic meter is 522 kg. In the mixing process, a pure source of water was utilized. The water-to-binder ratio was 0.38 in all mixtures.

Oxide composition	The percent by Weight (%)
(SiO_2)	20.36
(Al_2O_3)	3.65
(Fe_2O_3)	5.14
(CaO)	63.52
(MgO)	1.03
(SO_3)	2.23
(L.O.I)	4.24

Table 1: The chemical composition of OPC.

Test	Test result	E.S.S Limits
Specific gravity	3.15	-----
Specific surface area (gm/cm^2)	3298	≥ 2750
Setting time (min)	120	≥60 min
	360	≤10 hours
Pressure strength 2 days (MPa)	22.8	≥10 MPa
Pressure strength 28days (MPa)	57.2	≥42.5 MPa

Table 2: properties of OPC.

High-quality, impurity-free natural siliceous sand(S) was utilized as fine aggregate in the concrete mixtures. This study's fine aggregate was evaluated and verified to achieve the Egyptian Standards ES 1109-2008 [29]. The physical qualities of the sand used are shown in Tab. 3, and the sieve analysis of sand is displayed in Tab. 4.

Property	Sand	Limits*
Specific weight	2.5	-
Bulk density (gm/cm^3)	1.51	-
Fineness modulus	3	-
Material finer than No 200 sieve%	2.62	Less than 3%

*The limits according to Egyptian Specification No (1109/2008).

Table 3: The physical characteristics of the sand.

Sieve opening, mm	5	2.36	1.18	.6	.3	.15
Passing %	98.7	95.1	80.5	40.7	25.7	8.2

Table 4: Sieve analysis of sand.

In this investigation, dolomite (D), pumice (PC), and Addipore55 (AD) have been used as coarse aggregate types. The maximum nominal size of dolomite was 10 mm. The used dolomite was tested and verified to satisfy Egyptian Standards ES 1109-2008 [29]. Pumice is a natural aggregate available worldwide and is environmentally safe. When highly pressured materials are forcibly ejected from the volcano, PC is formed [30]. The properties of PC aggregate were examined following IS 2386 (Part 3 & 4)-1963 and IS 383–1970, based on the data sheet provided by the manufacturer, CEM company. Addipore55 is a light-weight aggregate with good thermal and acoustic properties, composed of expanded and extruded foam grains of a certain size and grade. The physical characteristics and particle size distributions of coarse aggregates are given in Tab. 5 and Fig. 1, respectively.

Property	Dolomite	Pumice	Addipore55
Specific weight	2.65	1.24	1.02
Bulk density (g/cm^3)	1.36	.49	.35
Grain size (mm)	12.5	8 -12	3-12
Water absorption%	0.65	2.5	1
Coefficient of impact %	24	50	-
Crushing value %	25	55	-

Table 5: The physical characteristics of coarse aggregate.

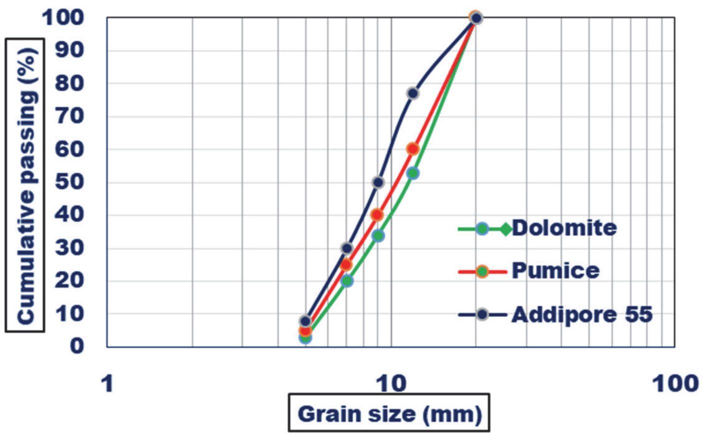

Figure 1: Particle size distributions of coarse aggregates.

In this study, two mineral additions were used as (PZ): silica fume (SF) and fly ash (FA), bought from Sika Egypt Company. As described on the manufacturer's datasheet, the physical composition of those used is shown in Tab. 6.

Property	SF	FA
Appearance / color	Light Gery powder	Gery fine powder
Surface area (g/cm^2)	170000	7000
Particle size, µm	8.00	10.00
Specific gravity	2.2	2.25

* According to the company's data sheet.

Table 6: The physical characteristics of mineral additions.

According to the Sika Egypt Company's manufacturer's data sheet, this study's fiber glass (FG) is a monofilament glass fiber sliced from E glass. The fiber is coated with salane-based sizing. The physical composition of the fiber glass used is shown in Tab. 7.

Property	Result*
Color	White
Design	Monofilament fiber
Fiber length	6mm
diameter	13±10% micron nominal

* According to the company's data sheet.

Table 7: The physical characteristics of fibre glass.

Addicrete BVF is a superplasticizer from CMB Company that complies with ASTM C 494 type F. It's a brown liquid colour with a density of 1.08 and the ratio of the Addicrete BVF to the cement was 2.5%.
In this study, two TADs were used; (AP) and (LC). They were obtained locally from Sika Egypt Company. Tab. 8 shows the physical characteristics of the AP. Also, the chemical compositions for AP were shown in Tab. 9, and the LC is a brownish liquid with a density of 1.01(Kg/lit), as given by the company's data sheet.

Property	Result*
Colour	Light Grey
Specific area (gm/cm^2)	11,340
Specific gravity	2.70

* According to the company's data sheet.

Table 8: The physical characteristics of AP.

Property	Result*
Chemical compositions (%)	12.846
(Al_2O_3)	85.637
(Fe_2O_3)	0.435
(CAO)	0.243
(TiO_2)	0.106

Table 9: The chemical composition of the used AP.

Mix design, mixing, casting procedure, and curing

Fourteen concrete mixes were prepared and tested with different content for four components (SF, FA, AP, and LC). The absolute volume method was used to calculate the weight of each ingredient required to make one cubic meter of concrete. Tab. 10 shows the concrete mix ratio and the weighted ingredients of the mixes. In all concrete mixes, 68.5% of the coarse aggregate was dolomite, while 28.5% was pumice, and 3% was addipore55. The coarse aggregate to sand ratio was 1:1 by weight. The SF (or FA) to cement ratio was 10%. The FG/cement ratio was 1%. The control mixes (M1 and M8) were made in the same way but without the addition of air agents.

Mix	SF/C	SF (kg/m³)	FA/C	FA (kg/m³)	AP/C	AP (kg/m³)	LC/C	LC (kg/m³)	S (kg/m³)	AD (kg/m³)	D (kg/m³)	PC (kg/m³)
M1	10%	58	0%	0	0%	0	0%	0	624.78	18.74	427.97	178.06
M2	10%	58	0%	0	0.25%	1.56	0%	0	624.15	18.72	427.54	177.88
M3	10%	58	0%	0	0.50%	3.12	0%	0	623.52	18.71	427.11	177.70
M4	10%	58	0%	0	0.75%	4.67	0%	0	622.89	18.69	426.68	177.52
M5	10%	58	0%	0	0%	0	0.25%	1.56	623.10	18.69	426.82	177.58
M6	10%	58	0%	0	0%	0	0.50%	3.11	621.43	18.64	425.68	177.11
M7	10%	58	0%	0	0%	0	0.75%	4.65	619.76	18.59	424.54	176.63
M8	0%	0	10%	58	0%	0	0%	0	625.42	18.76	428.41	178.24
M9	0%	0	10%	58	0.25%	1.56	0%	0	624.79	18.74	427.98	178.06
M10	0%	0	10%	58	0.5%	3.12	0%	0	624.16	18.72	427.55	177.88
M11	0%	0	10%	58	0.75%	4.68	0%	0	623.53	18.71	427.12	177.71
M12	0%	0	10%	58	0%	0	0.25%	1.56	623.73	18.71	427.26	177.76
M13	0%	0	10%	58	0%	0	0.5%	3.11	622.06	18.66	426.11	177.29
M14	0%	0	10%	58	0%	0	0.75%	4.65	620.40	18.61	424.97	176.81

Table 10: Mix ingredients.

This experimental work described the mixing process for fourteen concrete mixes in detail. First, determining amounts of cement and aggregate were mixed for two minutes in a mechanical mixer without water. The mixture was then blended with fine SF or FA on low speed for two minutes. Then, water and addicrete BVF were added into the mix for about four minutes till it was uniformly spread. Then, AP or LC was added. Finally, the FG was added according to ASTMC-192/C192M [31]. However, to evaluate the performance of the fresh concrete, the slump test was performed before boring the modules according to ASTM C143-78 [32]. The concrete mix was placed in moulds on three layers, and each layer was pressed with a vibration table for 30 seconds. One day after casting, the samples were extracted and placed in water-filled basins for use in the pressure test.

Compression strength test

Pressure tests were examined in the concrete laboratory of Tanta University's faculty of engineering using a hydraulic testing machine with a capacity of 2000 KN and an accuracy of 5 KN. All of the samples were extracted from the water basins and dried in the laboratory for nearly 2 hours before testing. The pressure strength was determined after 7, 28, and 90 days from casting according to BS EN 12390-3:2019 [33]. At each testing age, three specimen cubes (10×10×10 cm) from each mixture were examined, and the average was taken.

Density test

The density of the concrete was determined by using (10 x 10 x 10) cm cube samples after 28 days from casting age. The density was calculated according to ASTM C138/C138M-14 (2014), and the average of the three samples was taken.

Scanning electron microscope (SEM) analysis and energy-dispersive x-ray spectroscopy (eds)

The microstructure of five concrete mixes (M1, M2, M5, M9, and M12) was examined with a JEOL JSM-651OLV electronic microscope with a magnification capacity of 300,000 times. One magnification was chosen for specimen observation: 2000X. The procedure for preparing samples is detailed here. The examined concrete samples were collected from the inner core of the fractured specimens' outcome from compressive strength tests at the age of 90-days. The specimens were dried at 70 °C till they attained a consistent weight, then carbon glue was applied to the holders. A sputter coating evaporator coats gold on dried samples to get clearer and higher microstructure surface imaging. Also, (EDS) of type (Oxford X-Max 20) was used to identify the composition of the examined specimens.

X-ray diffraction (XRD)

The XRD technique was used to analyze cementitious materials, and anhydrous and hydrated cement phases at the age of 56 days. The tests were conducted at the Housing and Building National Research Center with an X-ray diffractometer type X'-Pert ProPhillips MPD PW 3050/60. Powder X-ray diffraction with a 0.154 nm filter was used for the XRD study, which was performed at room temperature.

Thermogravimetric analysis (TGA) and differential thermal analysis (DTG)

Thermogravimetric analysis (TGA) and Differential Thermal Analysis (DTG) were performed on mixes M1, M2, M5, M9, and M12 at the ages of 28, 56, and 90 days. About 50 mg of paste powder was tested, which was made with a water-to-binder ratio of 0.38 and stored at 20 °C in 20 mL sealed plastic jars. The paste was crushed into small pieces and immediately soaked in acetone to inhibit hydration and carbonization. After one day of curing in acetone, the samples were tested. Temperature peaks were observed. Most endothermic peaks are seen at their maximum temperature. In TGA testing, decreasing increments on TGA curves and endothermic peaks on the derived TGA indicated that cement hydrates were decomposing.

There are three stages in the breakdown of cement hydrates as follows [34,35]:

1-Evaporable water and calcium silicate hydrate decompose at temperatures ranging from 25 to 400 °C.

2-Calcium hydroxide(CH) (Ldx) decomposes at temperatures ranging from 400 to 600 °C.

3- Calcium carbonate decomposes to CaO and CO2 (Ldc) at temperatures ranging from 600 to 800 °C.

The first peak is divided into two regions with temperatures ranging from 25 to 400 °C. At temperatures ranging from 25 to 105 °C, the first phase corresponds to free water, whereas the dehydration process occurs at temperatures ranging from 105 to 400 °C (Ldh). The limited temperature is the most basic difference between free and chemically bound water.

RESULTS OF SLUMP TEST

Fig. 2 indicated that a higher slump equal to 365 mm was achieved in the mix (M11). However, a lower slump equal to 261 mm was achieved in the mix (M1). The use of AL with pozzolanic materials increased workability rather than LC. But, when different ratios of AL were applied, the workability decreased. This might be because of the consumption of free water during the AL reaction, which results in the formation of hydrogen gas bubbles [36].

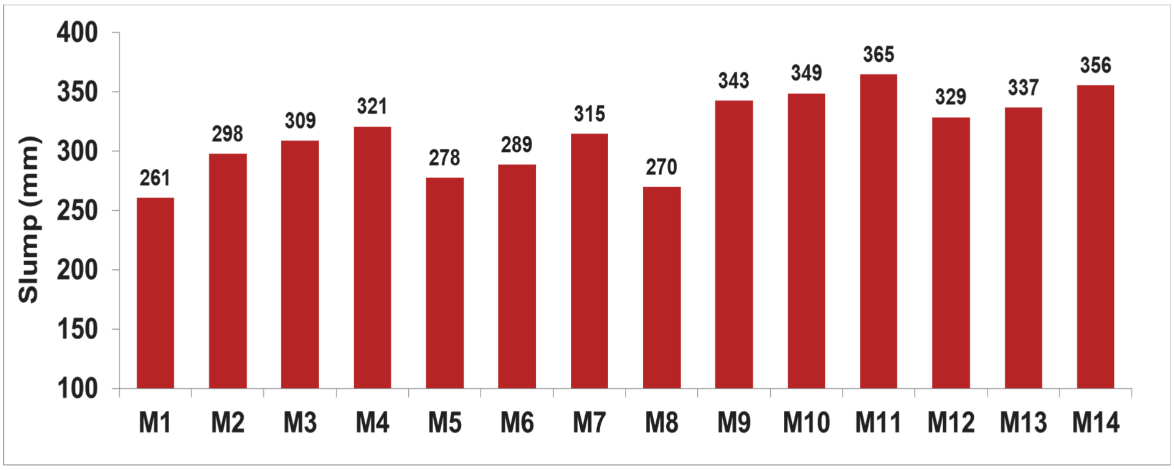

Figure 2: Slump of concrete mixtures.

RESULTS FOR THE SAMPLES UNDER PRESSURE

Figs. 3, 4, and 5 indicate the effects of TAD with (PZ) on the pressure strength (Fcu) of concrete after 7, 28, and 90 days of curing. The pressure strength of TAD in concrete was lower in all mixes when compared to non-TAD mixes.

Effect of trapped air addition content %

The pressure strength and porosity of concrete are inversely related; strength increases as the porosity of concrete decreases. Testing of concrete mixtures organized for this study using varying TAD ratios showed that those with a higher TAD ratio had a lower pressure strength. When compared (M1 and M8) with TAD mixes, the result indicated that higher pressure strength was achieved in mix M5, containing 0.25% LC and 10% SF, as shown in Fig. 3. On the other hand, a lower pressure strength was obtained by using AP in mix M11, which contains 0.75% AP and 10% FA. This reduction is caused by an increase in small bubbles in the wet mix containing the AL [37]. Also, these results support the theory that decreasing internal air content increases concrete pressure strength [38, 39].

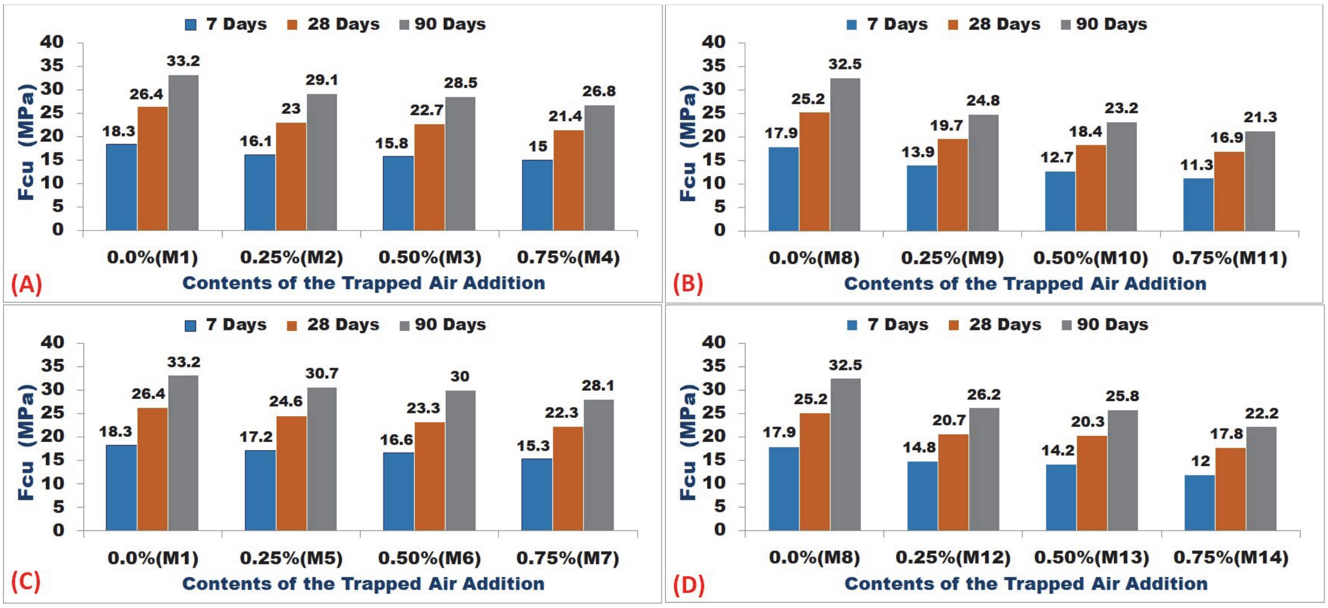

Figure 3: The effect of TAD contents on concrete pressure strength after 7 days, 28 days, and 90 days (A) for AP with 10% SF, (B) for AP with 10% FA, (C) for LC with 10% SF, and (D) for LC with 10% FA.

Effect of the Trapped Air Addition Type

As shown in Fig. 4, the results indicate a difference in pressure strength when the TAD type is changed from AP to LC. The LC type has a significantly higher effect on pressure strength than the AP type. Using 0.25% TAD and 10% SF, as shown in mixes M2 and M5, the pressure strength is equal to 1.6 MPa at 28 days and 1.6 MPa at 90 days. On the other hand, using 0.75% TAD and 10% SF, as shown in mixes M4 and M7, the gap in pressure strength is equal to 0.9 MPa at 28 days and 1.3 MPa at 90 days, respectively.

When using 0.25% TAD and 10% FA, as shown in mixes M9 and M12, the gap in pressure strength is equal to 1 MPa at 28 days and 1.4 MPa at 90 days, respectively. Also, when using 0.75% TAD and 10% FA, as shown in mixes M11 and M14, the difference in pressure strength is equal to 0.9 MPa at 28 days and 0.9 MPa at 90 days, respectively. Light-weight filler materials and foam agents for producing LWC increase porosity by providing many air gaps. As a result, the compressive strength is decreased [40, 41, 42].

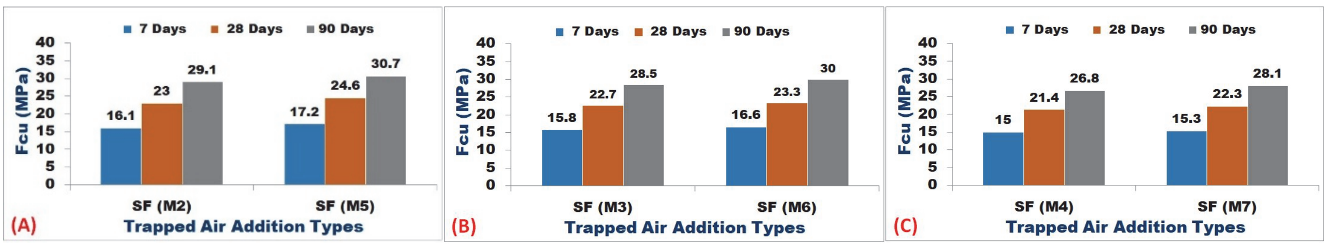

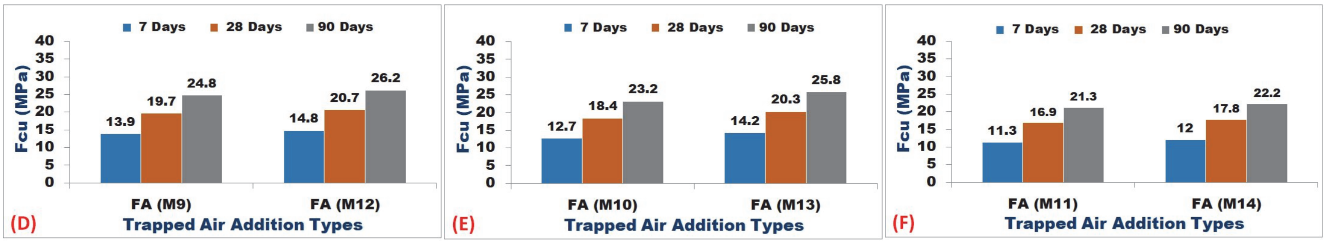

Figure 4: The effect of the TAD types on concrete pressure strength for samples at 7 days, 28 days, and 90 days was (A) 0.25% TAD with 10% SF; (B) 0.50% TAD with 10% SF; (C) 0.75% TAD with 10% SF; (D) 0.25% TAD with 10% FA; (E) 0.50% TAD with 10% FA; and (F) 0.75% TAD with 10% FA.

Effect of pozzolanic materials type

As shown in Fig. 5, the results indicate a difference in pressure strength when changing the type of pozzolan material from SF to FA. The SF type generally exceeds the FA type in terms of pressure strength. Using 10% (PZ) and 0% TAD, as shown in the mixes M1 and M8, the difference in pressure strength is equal to 1.2 MPA in 28 days and 0.7 MPA in 90 days. Furthermore, when 0.25% AP and 10% (PZ) are used, as shown in the mixes M2 and M9, the gap in pressure strength at 28 days is equal to 3.3 MPA and 4.3 MPA at 90 days. However, when 0.50% AP and 10% (PZ) are used, as shown in the mixes M3 and M10, the difference in pressure strength at 28 days is equal to 4.3 MPA and 5.3 MPA at 90 days, respectively. Furthermore, when 0.75% AP and 10% (PZ) are used, as shown in the mixes M4 and M11, the gap in pressure strength at 28 days is 4.5 MPA and 5.5 MPA at 90 days, respectively. This could be because control samples contain more C-S-H than other mixtures. PZ produces amorphous silica, which reacts with Ca(OH) 2, a byproduct of the Portland cement reaction, to produce more C-S-H. When TAD content is used, the pores in the structure become larger and more numerous[43].
However, when 0.25% LC and 10% (PZ) are used in mixes of M5 and M12, the gap in pressure strength at 28 days is equal to 3.9 MPa and 4.5 MPa at 90 days. When 0.50% LC and 10% (PZ) are used in mixes M6 and M13, the difference in pressure strength at 28 days is equal to 3 MPa and 4.2 MPa at 90 days. Furthermore, when using 0.75% LC and 10% (PZ) in mixes M7 and M14, the gap in pressure strength at 28 days is equal to 4.5 MPa and 5.9 MPa at 90 days, respectively. Other researchers reported that because the silica fume particles are in the pores as crystal seeds, and due to the effect of silica fume on the pozzolanic reaction, the hydration is carried out at a higher rate, forming more C-S-H gels [44, 45].

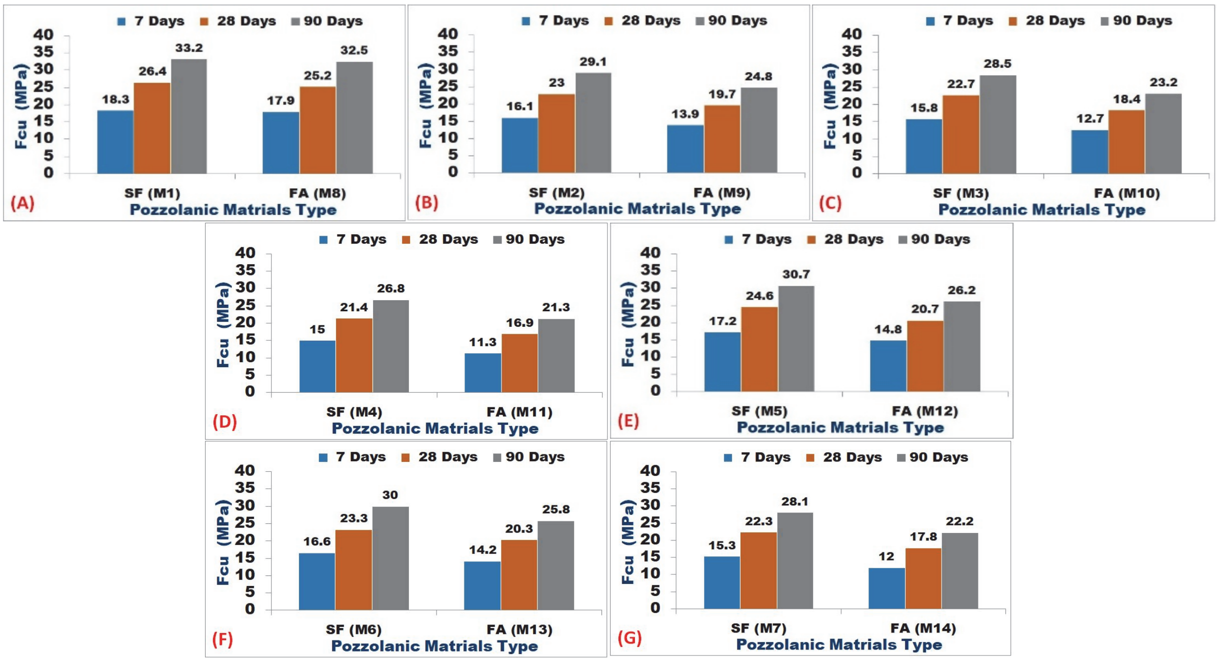

Figure 5: The effect of a 10% pozzolanic material types on concrete pressure strength at 7, 28, and 90 days (A) 0.0% TAD; (B) 0.25% AP; (C) 0.50% AP; (D) 0.75% AP; (E) 0.25% LC; (F) 0.50% LC; (G) 0.75% LC.

Results for the specimens under the density test

Fig. 6 indicated that a higher pressure strength of 26.4 mpa with a higher density of 1770 kg/m³ was achieved in the mix (M1). However, a lower pressure strength of 16.9 mpa with a lower density of equal to 1347 kg/m³ was achieved in the mix (M11). This might be due to the development of hydrogen gas and the production of air gaps when AL is combined with cementitious material [46]. Other researchers reported that, as the concrete density decreased, the pressure strength also decreased [47, 48, 49].

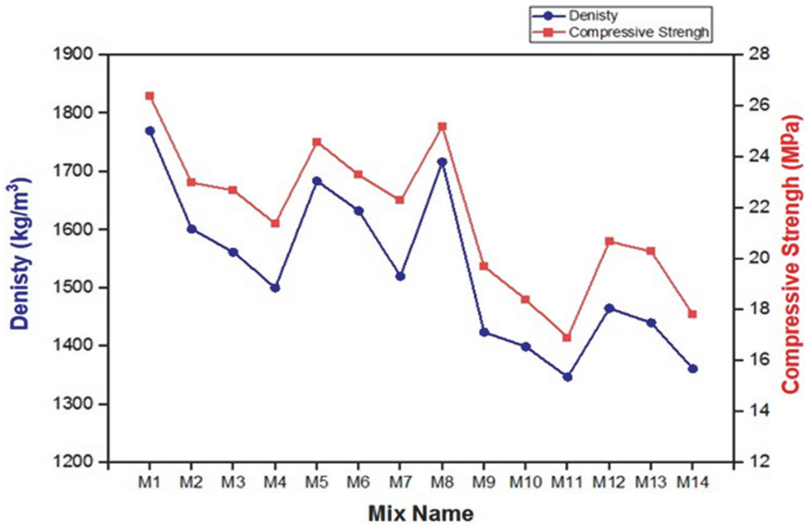

Figure 6: The relationship between the density and the pressure strength at 28 days.

SEM, EDS, XRD, TGA, and DTG results

Scanning Electron Microscope (SEM)

SEM is used to examine specimens of TAD concrete mixes and control concrete mixes for signs of microbial calcium silicate hydrate precipitation and voids. The SEM test compares mixes M2, M5, M9, and M12 to control mix M1. Figs. 7 show the results. After 90 days of curing, SEM examinations were performed at magnifications of 2000X. The examined TAD specimens revealed more voids than the control mix, according to the observations. This might be because when the TAD combines with the silica, millions of small hydrogen bubbles occur[50]. Also, control specimens had more calcium silicate hydrate than other mixes. Additionally, TAD specimens had less intense microstructures than the control mix. This indicates that increasing the trapped air content causes an increase in the voids of the concrete matrix and a decrease in the production of CH crystals [51, 52, 53].

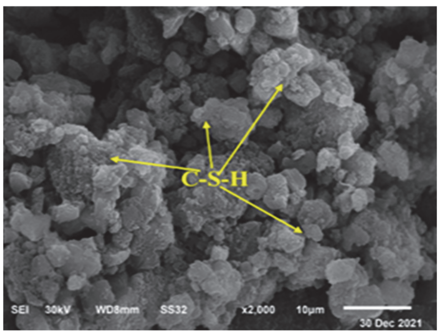

(1)

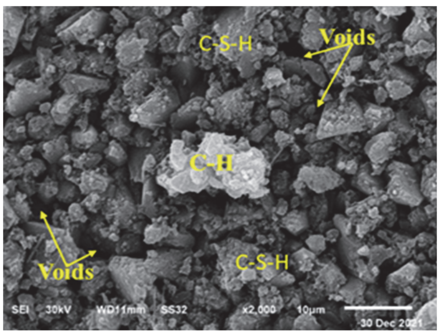

(2)

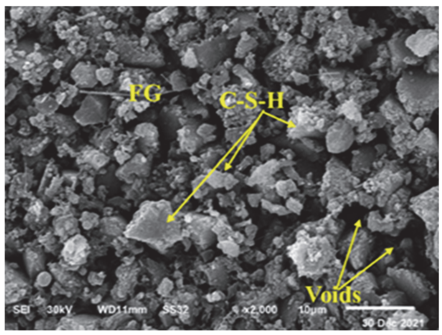

(3)

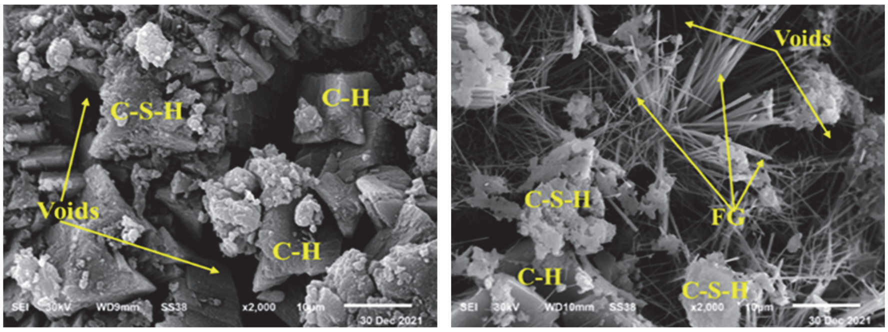

(4) (5)

Figure 7: SEM test for 5 concrete mixtures after 90 days of processing (1) M1, (2) M2, (3) M5, (4) M9, and (5) M12.

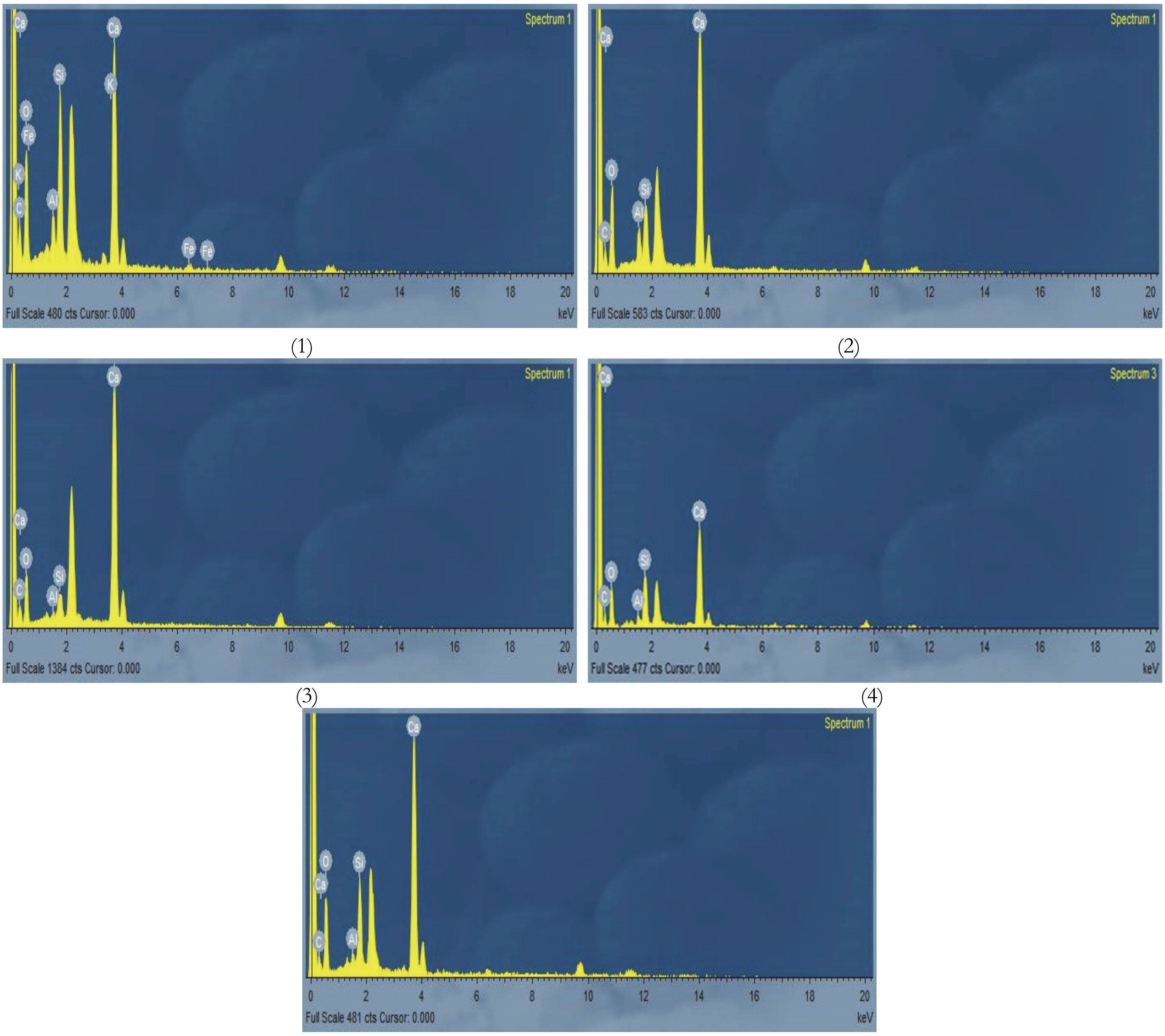

(1) (2) (3) (4) (5)

Figure 8: EDS spectra for 5 mixtures: (1) M1, (2) M2, (3) M5, (4) M9, and (5) M12 to indicate the Ca/Si ratio in each mix.

Energy dispersive spectrometer (EDS)

Fig. 8 depicts the results of EDS. It was used to check the peaks of the chemical components shown in the specimens of five mixtures. The major components of mixtures are Calcium carbonate (C), Oxygen (O), Aluminium oxide (Al), Silicon dioxide (Si), and Wollastonite (Ca). The results also showed that Wollastonite peaks appeared in all samples, but Wollastonite peaks appeared in lower quantities in TAD mixtures compared to the control mix. The atomic percentage of Ca/Si tested mixtures is one of the main indicators observed, as shown in Tab. 11. According to EDS findings, the atomic Ca/Si ratios for M1, M2, M5, M9, and M12 are equal to 1.45, 2.26, 2.11, 4.67, and 3.02, respectively. Other research reports that concrete mixtures with higher compressive strength have a lower Ca/Si ratio [54, 55, 41].

Element	Mix M1		M2		M5		M9		M12	
	Weight %	Atomic %	Weight %	Atomic %	Weight %	Atomic %	Weight %	Atomic %	Weight %	Atomic %
C K	8.17	13.41	11.31	25.11	22.74	33.58	11.06	17.79	12.11	19.34
O K	52.17	64.32	40.42	45.50	45.83	50.80	52.14	62.94	51.39	61.62
Al K	2.84	2.08	2.06	1.66	1.40	0.92	2.65	1.90	0.88	0.63
Si K	10.92	7.67	10.92	8.49	7.47	4.72	4.45	3.06	6.70	4.58
Ca K	22.71	11.18	35.30	19.23	22.56	9.98	29.69	14.31	28.91	13.84

Table 11: EDS analysis for control mix and TAD mixes.

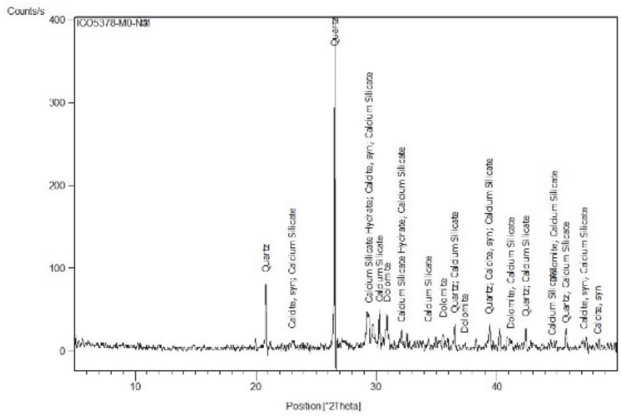

(1)

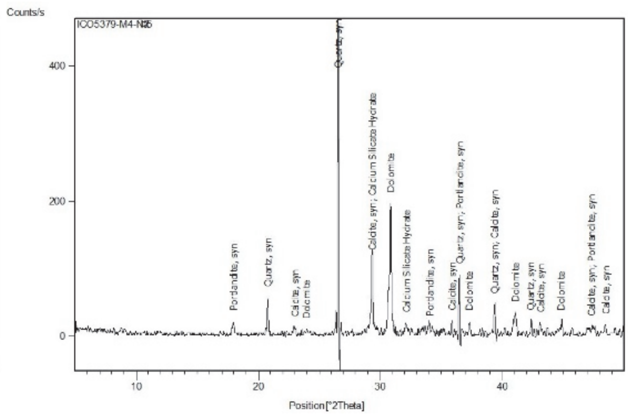

(2)

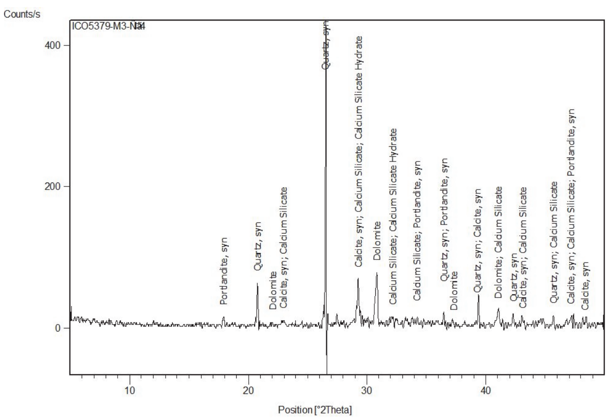

(3)

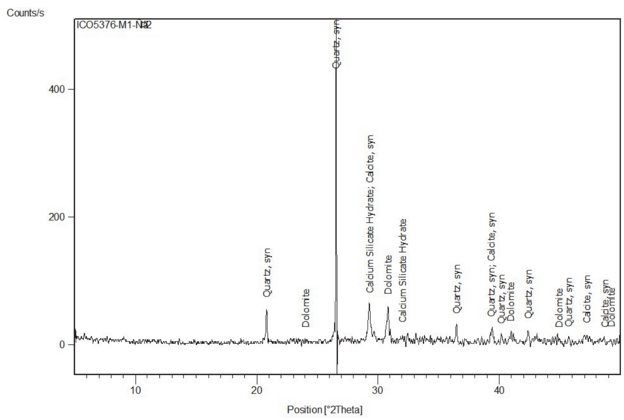

(4)

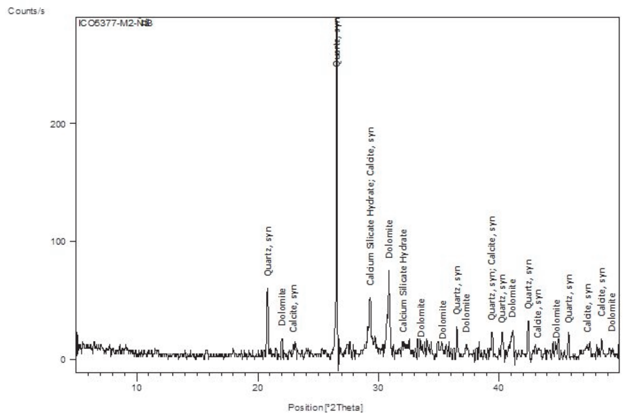

(5)

Figure 9: X- ray diffraction for 5 concrete mixtures after 90 days of processing (1) M1, (2) M2, (3) M5, (4) M9, and (5) M12.

X-ray diffraction

Fig. 9 shows the XRD patterns of concrete mixtures (M1, M2, M5, M9, and M12) at 56 days. Potolandite, calcium silicate hydrate, calcium silicate, calcite, and quarts are the main components of concrete mixtures. Potolandite peaks appeared in mixtures M2 and M5. On the other hand, calcium silicate hydrate is higher in mix M1 than in TAD mixes. Also, calcium silicate peaks appeared in M1 and M5. Calcite peaks were found in the samples. This may mean that the calcite is produced from the sand and coarse material used. Peaks of quartz diffraction were found in TAD samples greater than M1. This could be because of the TAD producing air voids. The use of quartz is also affected by trapped air content [17, 56, 57].

Thermogravimetric analysis (TGA) and differential thermal analysis (DTG)

The degree of hydration of different mixes shown in Fig. 10 was chemically calculated using thermogravimetric analysis (TGA) on cement pastes, which was determined by the mass difference between 25 and 1000 °C as [30]. Free water and C-S-H gel dehydration are responsible for the weight loss below 400 °C, which corresponds to the first main endothermic peak. At temperatures of between 600 and 800 °C, weight loss occurs, which corresponds to the decomposition of ill-crystalline calcium carbonate. The TGA/DTG curves of M1, M2, M5, M9, and M12 samples at the ages of 28 and 90 days are shown in Fig. 11. In the short term, the hydration degree of mix M1 cement paste grew at a faster rate than the other mixes. The degree of hydration at 28, 56, and 90 days was 49.02%, 52.77%, and 55.19%, respectively. The results showed that using SF with TAD to pastes improved the hydration kinetics significantly compared with FA. Also, as compared to the control mix, adding 10% SF with 0.25%LC in mix M5 decreased the degree of hydration by 1.46%, 1.36%, and 0.67% for 28, 56, and 90 days, respectively. Similarly, compared to the control mix, using 10% FA with 0.25 % LC in M12 paste reduced hydration by 4.5%, 4.18 %, and 3.51 % at 28, 56, and 90 days. As a consequence, TGA measurements revealed that utilizing SF as a cementitious material at a content of 10% produced the same CH and CSH content. This would prove that it has similar good pozzolanic activity [56].

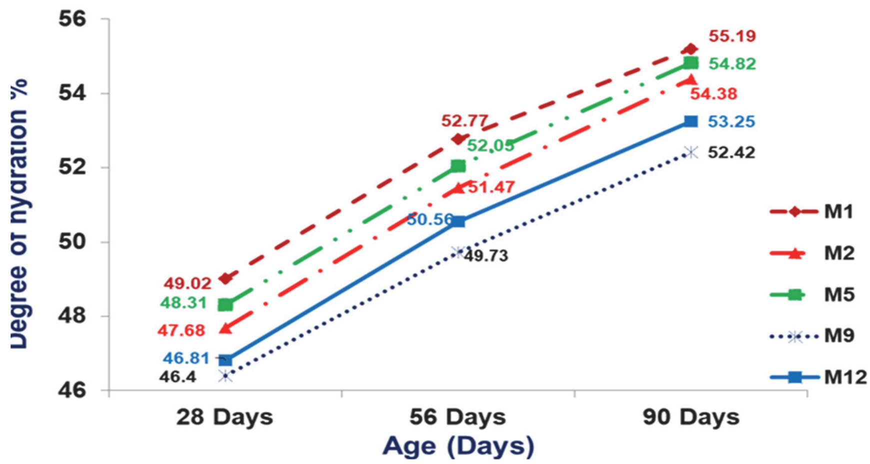

Figure 10: Cement paste hydration degree evaluation.

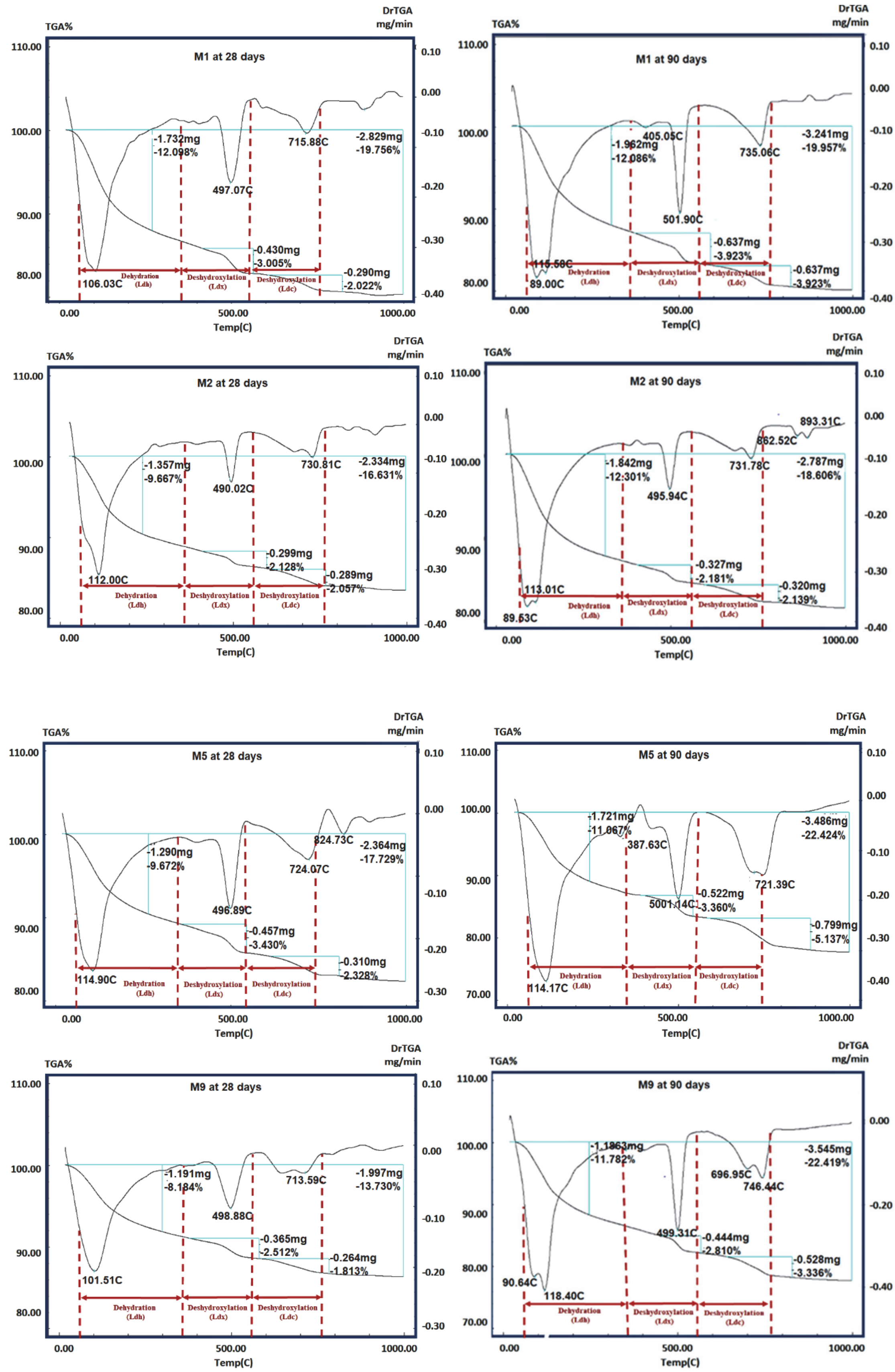
M1 at 28 days
M1 at 90 days
M2 at 28 days
M2 at 90 days
M5 at 28 days
M5 at 90 days
M9 at 28 days
M9 at 90 days
TGA%
DrTGA
mg/min
Temp(C)
Dehydration
(Ldh)
Deshydroxylation
(Ldx)
Deshydroxylation
(Ldc)
106.03C
497.07C
715.88C
-1.732mg
-12.098%
-0.430mg
-3.005%
-0.290mg
-2.022%
-2.829mg
-19.756%
89.00C
115.58C
405.05C
501.90C
735.06C
-1.962mg
-12.086%
-0.637mg
-3.923%
-3.241mg
-19.957%
112.00C
490.02C
730.81C
-1.357mg
-9.667%
-0.299mg
-2.128%
-0.289mg
-2.057%
-2.334mg
-16.631%
89.63C
113.01C
495.94C
731.78C
862.52C
893.31C
-1.842mg
-12.301%
-0.327mg
-2.181%
-0.320mg
-2.139%
-2.787mg
-18.606%
114.90C
496.89C
724.07C
824.73C
-1.290mg
-9.672%
-0.457mg
-3.430%
-0.310mg
-2.328%
-2.364mg
-17.729%
114.17C
387.63C
721.39C
-1.721mg
-11.067%
-0.522mg
-3.360%
-0.799mg
-5.137%
-3.486mg
-22.424%
101.51C
498.88C
713.59C
-1.191mg
-8.184%
-0.365mg
-2.512%
-0.264mg
-1.813%
-1.997mg
-13.730%
90.64C
118.40C
499.31C
696.95C
746.44C
-1.1863mg
-11.782%
-0.444mg
-2.810%
-0.528mg
-3.336%
-3.545mg
-22.419%

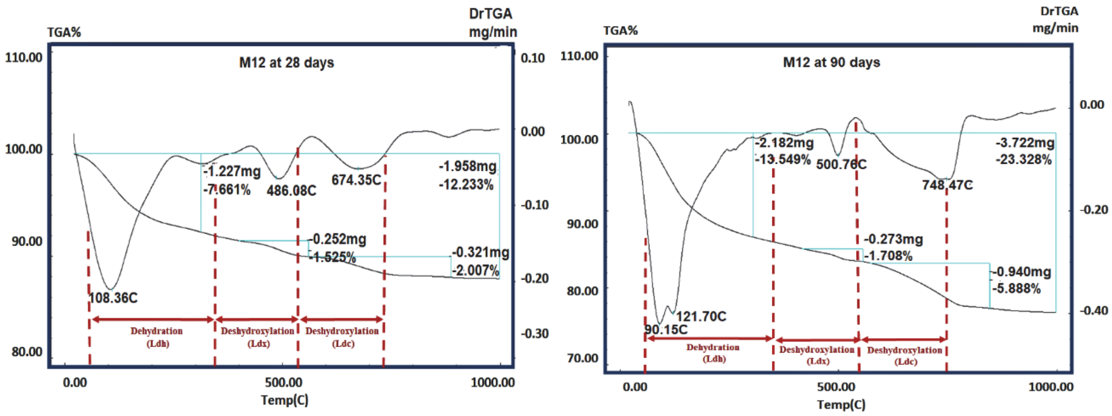

Figure 11: TGA/DTG of cement paste of mixes (M1, M2, M5, M9, and M12).

Conclusions

In this work, we focused on the characteristics of LWC, which was made by combining pumice and addipore as light-weight aggregates with AL and LC as TAD. SF and FA were also used as pozzolanic material. The TAD type, TAD content, and pozzolanic material type were all examined. The compressive strength test findings were also confirmed by investigating the microstructure characteristics of concrete using SEM, EDS, XRD, and TGA. Based on the findings of this study, the following conclusions can be drawn:

1-The mixes containing SF have a higher compressive strength than those containing FA.

2-The highest compressive strength was achieved using SF followed by FA, without any air additives in either case.

3-When utilizing air additives with pozzolanic material, the higher compressive strength was achieved using 0.25% LC, followed by 0.50% LC, 0.25% AL, 0.50% AL, and 0.75% LC, respectively.

4- The result indicated that raising the TAD ratio reduced the compressive strength and density of concrete. Using 0.75% AL with FA, a pressure of 16.9 mpa with a density of 1347 kg/m^3 was achieved in the mix (M11). Also, using 0.75% LC with FA, a pressure of 17.8 mpa with a density of 1361 kg/m^3 was achieved in the mix (M14).

5-Using 28.5% pumice and 3% addipore 55 as a light-weight aggregate, the density decreases from 1770 kg/m3 to 1347 kg/m^3.

6- The SEM and EDS studies indicated that the production of calcium silicate hydrate (CSH) was decreased, while the pores and air voids increased.

7-TGA/DTG tests revealed that the hydration degree of the mix without TAD cement paste grew at a faster rate than the other mixes.

References

[1] Alqahtani, F.K. (2022). Technical Assessment of Green lightweight concrete containing manufactured plastic aggregates. Journal of Building Engineering, 50, p.104169. DOI: 10.1016/j.jobe.2022.104169.

[2] Bamigboye, G.O., Tarverdi, K., Umoren, A., Bassey, D.E., Okorie, U. and Adediran, J. (2021). Evaluation of eco-friendly concrete having waste PET as fine aggregates. Cleaner Materials, 2, p.100026. DOI: 10.1016/j.clema.2021.100026.

[3] Del Rey Castillo, E., Almesfer, N., Saggi, O. and Ingham, J.M. (2020). Light-weight concrete with artificial aggregate manufactured from plastic waste. Construction and Building Materials, 265, p.120199. DOI: 10.1016/j.conbuildmat.2020.120199.

[4] Záleská, M., Pavlíková, M., Pokorný, J., Jankovský, O., Pavlík, Z. and Černý, R. (2018). Structural, mechanical and hygrothermal properties of lightweight concrete based on the application of waste plastics. Construction and Building Materials, 180, pp.1-11. DOI:10.1016/j.conbuildmat.2018.05.250.

[5] Almeshal, I., Tayeh, B.A., Alyousef, R., Alabduljabbar, H. and Mohamed, A.M. (2020). Eco-friendly concrete containing recycled plastic as partial replacement for sand. Journal of Materials Research and Technology, 9(3), pp. 4631-4643. DOI: 10.1016/j.jmrt.2020.02.090.

[6] Gao, H., Wang, W., Liao, H. and Cheng, F. (2021). Characterization of light foamed concrete containing fly ash and desulfurization gypsum for wall insulation prepared with vacuum foaming process. Construction and Building Materials, 281, p.122411. DOI: 10.1016/j.conbuildmat.2021.122411.

[7] Zhang, X., Yang, Q., Shi, Y., Zheng, G., Li, Q., Chen, H. and Cheng, X. (2020). Effects of different control methods on the mechanical and thermal properties of ultra-light foamed concrete. Construction and Building Materials, 262, p.120082. DOI: 10.1016/j.conbuildmat.2020.120082.

[8] Bagheri, A. and Samea, A. (2019). Effect of air content on the rheology of foamed concrete. Magazine of Concrete Research, 71(9), pp.461-467. DOI: 10.1680/jmacr.17.00267.

[9] Kumar, V.K., Priya, A.K., Manikandan, G., Naveen, A.S., Nitishkumar, B. and Pradeep, P. (2021). Review of materials used in light weight concrete. Materials Today: Proceedings, 37, pp. 3538-3539. DOI: 10.1016/j.matpr.2020.09.425.

[10] Bejan, G., Bărbuță, M., Vizitiu, R.Ș. and Burlacu, A. (2020). Lightweight concrete with waste-review. Procedia Manufacturing, 46, pp. 136-143. DOI: 10.1016/j.promfg.2020.03.021.

[11] Krishna, A.S., Siempu, R. and Kumar, G.S. (2021). Study on the fresh and hardened properties of foam concrete incorporating fly ash. Materials Today: Proceedings, 46, pp. 8639-8644. DOI: 10.1016/j.matpr.2021.03.599.

[12] Elango, K.S., Sanfeer, J., Gopi, R., Shalini, A., Saravanakumar, R. and Prabhu, L. (2021). Properties of light weight concrete–a state of the art review. Materials Today: Proceedings, 46, pp.4059-4062. DOI: 10.1016/j.matpr.2021.02.571.

[13] Hashim, M. and Tantray, M. (2021). Comparative study on the performance of protein and synthetic-based foaming agents used in foamed concrete. Case Studies in Construction Materials, 14, p.e00524. DOI: 10.1016/j.cscm.2021.e00524.

[14] Kozłowski, M. and Kadela, M. (2018). Mechanical characterization of lightweight foamed concrete. Advances in Materials Science and Engineering. DOI: 10.1155/2018/6801258.

[15] Ke, G., Zhang, J., Tian, B. and Wang, J. (2020). Characteristic analysis of concrete air entraining agents in different media. Cement and Concrete Research, 135, p.106142. DOI: 10.1016/j.cemconres.2020.106142.

[16] Leong, G.W., Chin, T.M., Mo, K.H., Ibrahim, Z., Putra, A. and Othman, M.N. (2021). Incorporation of crumb rubber and air-entraining agent in ultra-lightweight cementitious composite: Evaluation of mechanical and acoustic properties. Journal of Building Engineering, 42, p.103034. DOI: 10.1016/j.jobe.2021.103034.

[17] Al-kroom, H., Atyia, M.M., Mahdy, M.G. and Abd Elrahman, M. (2022). The Effect of Finely-Grinded Crushed Brick Powder on Physical and Microstructural Characteristics of Lightweight Concrete. Minerals, 12(2), p.159. DOI: 10.3390/min12020159.

[18] Ahmad, M.R. and Chen, B. (2019). Experimental research on the performance of lightweight concrete containing foam and expanded clay aggregate. Composites Part B: Engineering, 171, pp.46-60. DOI: 10.1016/j.compositesb.2019.04.025.

[19] Kim, H.K., Jeon, J.H. and Lee, H.K. (2012). Workability, and mechanical, acoustic and thermal properties of lightweight aggregate concrete with a high volume of entrained air. Construction and Building Materials, 29, pp. 193-200. DOI: 10.1016/j.conbuildmat.2011.08.067.

[20] Hosen, M.A., Shammas, M.I., Shill, S.K., Jumaat, M.Z., Alengaram, U.J., Ahmmad, R., Althoey, F., Islam, A.S. and Lin, Y. (2021). Investigation of structural characteristics of palm oil clinker based high-strength lightweight concrete comprising steel fibers. Journal of Materials Research and Technology, 15, pp. 6736-6746. DOI: 10.1016/j.jmrt.2021.11.105.

[21] Ding, F., Wu, X., Xiang, P. and Yu, Z. (2021). New damage ratio strength criterion for concrete and lightweight aggregate concrete. ACI Structural Journal, 118(6), pp.165-178. DOI: 10.14359/51732989.

[22] Wu, T., Sun, Y., Liu, X. and Cao, Y. (2021). Comparative study of the flexural behavior of steel fiber-reinforced lightweight aggregate concrete beams reinforced and prestressed with CFRP tendons. Engineering Structures, 233, p.111901. DOI: 10.1016/j.engstruct.2021.111901.

[23] Deifalla, A. (2020). Torsion design of lightweight concrete beams without or with fibers: A comparative study and a refined cracking torque formula. Structures, 28, pp. 786-802. DOI: 10.1016/j.istruc.2020.09.004.

[24] Nawaz, W., Abdalla, J.A., Hawileh, R.A., Alajmani, H.S., Abuzayed, I.H., Ataya, H. and Mohamed, H.A. (2019). Experimental study on the shear strength of reinforced concrete beams cast with Lava lightweight aggregates. Archives of Civil and Mechanical Engineering, 19(4), pp. 981-996. DOI: 10.1016/j.acme.2019.05.003.

[25] Wang, Z., Li, X., Jiang, L., Wang, M., Xu, Q. and Harries, K. (2020). Long-term performance of lightweight aggregate reinforced concrete beams. Construction and Building Materials, 264, p.120231. DOI: 10.1016/j.conbuildmat.2020.120231.

[26] Dabbaghi, F., Fallahnejad, H., Nasrollahpour, S., Dehestani, M. and Yousefpour, H. (2021). Evaluation of fracture energy, toughness, brittleness, and fracture process zone properties for lightweight concrete exposed to high temperatures. Theoretical and Applied Fracture Mechanics, 116, p.103088. DOI: 10.1016/j.tafmec.2021.103088.
[27] Solak, A.M., Tenza-Abril, A.J. and García-Vera, V.E. (2022). Adopting an image analysis method to study the influence of segregation on the compressive strength of lightweight aggregate concretes. Construction and Building Materials, 323, p.126594. DOI: 10.1016/j.conbuildmat.2022.126594.
[28] Egyptian Standard Specification, Cement – Physical and Mechanical Tests (2005)/ESS 2421.
[29] E.S.S. No. 1109, (2008) "Aggregate", Egyptian Standard Specification, Ministry of Industry, Cairo, Egypt.
[30] Karthika, R.B., Vidyapriya, V., Sri, K.N., Beaula, K.M.G., Harini, R. and Sriram, M., (2021). Experimental study on lightweight concrete using pumice aggregate. Materials Today: Proceedings, 43, pp. 1606-1613. DOI: 10.1016/j.matpr.2020.09.762.
[31] Standards American Society for Testing and Materials 4(2), Standard Practice for Making and Curing Concrete Test Specimens in the Laboratory Annual Book of ASTM, ASTM (2015), C192/C192M
[32] Standard Test Method for Slump Of Portland Cement Concrete.
[33] British Standards Institution, Testing hardened concrete-part 3: compressive strength of test specimens, BS EN (2019),12390-3.
[34] Deboucha, W., Leklou, N., Khelidj, A. and Oudjit, M.N. (2017). Hydration development of mineral additives blended cement using thermogravimetric analysis (TGA): Methodology of calculating the degree of hydration. Construction and Building Materials, 146, pp. 687-701. DOI: 10.1016/j.conbuildmat.2017.04.132.
[35] Scrivener, K., Snellings, R. and Lothenbach, B. eds. (2016). A practical guide to microstructural analysis of cementitious materials (Vol. 540). Boca Raton, FL, USA, Crc Press. DOI: 10.1201/b19074.
[36] Yoon, J., Kim, H., Koh, T. and Pyo, S. (2020). Microstructural characteristics of sound absorbable porous cement-based materials by incorporating natural fibers and aluminum powder. Construction and Building Materials, 243, p.118167. DOI: 10.1016/j.conbuildmat.2020.118167.
[37] Thakur, A. and Kumar, S. (2022). Mechanical properties and development of light weight concrete by using autoclaved aerated concrete (AAC) with aluminum powder. Materials Today: Proceedings, 56, pp. 3734-3739. DOI: 10.1016/j.matpr.2021.12.508.
[38] Özcan, F. and Koc, M.E. (2018). Influence of ground pumice on compressive strength and air content of both non-air and air entrained concrete in fresh and hardened state. Construction and Building Materials, 187, pp. 382-393. DOI: 10.1016/j.conbuildmat.2018.07.183.
[39] Beghoura, I. and Castro-Gomes, J. (2019). Design of alkali-activated aluminium powder foamed materials for precursors with different particle sizes. Construction and Building Materials, 224, pp. 682-690. DOI: 10.1016/j.conbuildmat.2019.07.018.
[40] Zhang, Z., Yuvaraj, A., Di, J. and Qian, S. (2019). Matrix design of light weight, high strength, high ductility ECC. Construction and Building Materials, 210, pp. 188-197. DOI: 10.1016/j.conbuildmat.2019.03.159.
[41] Xiong, Y., Zhu, Y., Chen, C. and Zhang, Y. (2021). Effect of nano-alumina modified foaming agents on properties of foamed concrete. Construction and Building Materials, 267, p.121045. DOI: 10.1016/j.conbuildmat.2020.121045.
[42] Falliano, D., De Domenico, D., Ricciardi, G. and Gugliandolo, E. (2018). Experimental investigation on the compressive strength of foamed concrete: Effect of curing conditions, cement type, foaming agent and dry density. Construction and Building Materials, 165, pp. 735-749. DOI: 10.1016/j.conbuildmat.2017.12.241.
[43] Van, L.T., Kim, D.V., Xuan, H.N., Dinh, T.V., Bulgakov, B. and Bazhenova, S. (2019. Effect of aluminium powder on light-weight aerated concrete properties. In E3S Web of Conferences 97, p. 0200. EDP Sciences. DOI: 10.1051/e3sconf/20199702005.
[44] Wang, X., Huang, J., Dai, S., Ma, B. and Jiang, Q. (2020). Investigation of silica fume as foam cell stabilizer for foamed concrete. Construction and Building Materials, 237, p.117514. DOI: 10.1016/j.conbuildmat.2019.117514.
[45] Gökçe, H.S., Hatungimana, D. and Ramyar, K. (2019). Effect of fly ash and silica fume on hardened properties of foam concrete. Construction and building materials, 194, pp.1-11. DOI: 10.1016/j.conbuildmat.2018.11.036.
[46] Song, Y., Li, B., Yang, E.H., Liu, Y. and Chen, Z. (2016). Gas generation from incinerator bottom ash: potential aerating agent for lightweight concrete production. Journal of Materials in Civil Engineering, 28(7), p. 04016030. DOI: 10.1061/(asce)mt.1943-5533.0001524.
[47] Kumar, N.V., Arunkumar, C. and Senthil, S.S. (2018). Experimental study on mechanical and thermal behavior of foamed concrete. Materials Today: Proceedings, 5(2), pp. 8753-8760. DOI: 10.1016/j.matpr.2017.12.302.

[48] Olofinnade, O., Chandra, S. and Chakraborty, P. (2021). Recycling of high impact polystyrene and low-density polyethylene plastic wastes in lightweight based concrete for sustainable construction. Materials Today: Proceedings, 38, pp. 2151-2156. DOI: 10.1016/j.matpr.2020.05.176.
[49] Schumacher, K., Saßmannshausen, N., Pritzel, C. and Trettin, R. (2020). Lightweight aggregate concrete with an open structure and a porous matrix with an improved ratio of compressive strength to dry density. Construction and Building Materials, 264, p. 120167. DOI: 10.1016/j.conbuildmat.2020.120167.
[50] Rafiza, A.R., Fazlizan, A., Thongtha, A., Asim, N. and Noorashikin, M.S. (2022). The Physical and Mechanical Properties of Autoclaved Aerated Concrete (AAC) with Recycled AAC as a Partial Replacement for Sand. Buildings, 12(1), p.60. DOI: 10.3390/buildings12010060.
[51] Hou, L., Li, J., Lu, Z. and Niu, Y. (2021). Influence of foaming agent on cement and foam concrete. Construction and Building Materials, 280, p.122399. DOI: 10.1016/j.conbuildmat.2021.122399.
[52] Pundienė, I., Pranckevičienė, J., Kligys, M. and Kizinievič, O. (2020). The synergetic interaction of chemical admixtures on the properties of eco-friendly lightweight concrete from industrial technogenic waste. Construction and Building Materials, 256, p.119461. DOI: 10.1016/j.conbuildmat.2020.119461.
[53] Xie, J., Liu, J., Liu, F., Wang, J. and Huang, P. (2019). Investigation of a new lightweight green concrete containing sludge ceramsite and recycled fine aggregates. Journal of Cleaner Production, 235, pp. 1240-1254. DOI: 10.1016/j.jclepro.2019.07.012.
[54] Sahu, S.S. and Gandhi, I.S.R. (2021). Studies on influence of characteristics of surfactant and foam on foam concrete behaviour. Journal of Building Engineering, 40, p.102333. DOI: 10.1016/j.jobe.2021.102333.
[55] Kunther, W., Ferreiro, S. and Skibsted, J. (2017). Influence of the Ca/Si ratio on the compressive strength of cementitious calcium–silicate–hydrate binders. Journal of Materials Chemistry A, 5(33), pp.17401-17412. DOI: 10.1039/c7ta06104h.
[56] Atyia, M.M., Mahdy, M.G. and Abd Elrahman, M. (2021). Production and properties of lightweight concrete incorporating recycled waste crushed clay bricks. Construction and Building Materials, 304, p.124655. DOI: 10.1016/j.conbuildmat.2021.124655.
[57] Arifullah, S.M. and Madhavi, Y. (2021). Micro structural examination of low-density light weight concrete based on expanded polypropylene foam. Materials Today: Proceedings. DOI: 10.1016/j.matpr.2020.11.564.